Fracture Mechanics of Concrete and Concrete Structures -
Recent Advances in Fracture Mechanics of Concrete - B. H. Oh, et al.(eds)
ⓒ 2010 Korea Concrete Institute, Seoul, ISBN 978-89-5708-180-8

Combined approach based on the mechanical behavior and microstructural examinations for the fracture of concrete

H. Yildirim, O.N. Oktar, Y. Akkaya, O. Sengul & M.A. Tasdemir
Istanbul Technical University, Faculty of Civil Engineering, Istanbul, Turkey

ABSTRACT: Investigations on the uniaxial compressive behavior of concretes made with two different aggregates such as rounded siliceous gravel and crushed limestone under short-term loading are reported. For each aggregate type, maximum particle size, the grading and water-cement ratio of concretes were kept constant, and the aggregate volume fraction was varied from 0 (hcp) to 0.73 m^3/m^3 (concrete). For better understanding of the fracture properties and crack initiation and propagation in concretes with two different coarse aggregates, a microstructural examination method using optical fluorescence are also presented. Test results indicate that, in gravel concretes the compressive strength and critical stresses (i.e. discontinuity and loosening limits) gradually decrease with increasing aggregate volume fraction. On the other hand, in crushed limestone concretes, the decrease is observed to about 0.40 m^3/m^3 of aggregate concentration, then the compressive strength and critical stresses increase with increasing aggregate volume fraction. Good agreement was found between the results obtained and the microstructural investigations.

1 INTRODUCTION

In recent years, research on concrete has primarily concentrated on increasing its compressive strength and also durability, however, more information is needed for many aspects of mechanical properties such as tensile properties and fracture behavior (Konsta-Gdoutos 2006).

When the hardened cement paste or the parent rock which the aggregates are obtained from, are subjected to uniaxial compression, they exhibit elastic behavior, but inelastic behavior is obtained for concrete. At microstructural level, concrete is a highly heterogeneous material consisting of coarse and fine aggregates, hardened cement paste, interface between the aggregates and paste, and also voids and microcracks (Shah & Tasdemir 1994). Aggregate – cement interfacial zone is considered the weakest link in concrete. Oriented large crystals of CH constitute an important part of this region and the porosity of the interface is also higher compared to the bulk paste. As a result, the interface is susceptible to cracking and microcracking to occur due to shrinkage or thermal effects. It is known that the inelastic behavior of concrete is related to the internal microcracking. Studies conducted using microscopic analysis and holographic interferometry have revealed that cracks in concrete initiate at the interface and then propagate into the matrix (Tasdemir et al. 1990, Jensen & Chatterji 1996).

In recent years, the effects of aggregate type and size of aggregate on the mechanical behavior of concrete were investigated by several researchers (Tasdemir et al. 1999). One of the main toughening mechanisms in concrete is aggregate bridging; it occurs when the crack advances beyond an aggregate to transmit the stress across the crack resulting in grain pullout. This mechanism causes energy dissipation through friction (Shah et al. 1995). A limited amount of information, however, is available on the effect of aggregate volume fraction on the fracture properties of concrete (Tasdemir & Karihaloo 2001).

One of the methods for the investigation of microstructure is the visual examination by plane and thin section analysis. The method used in concrete microstructure has been borrowed from geology and it is based on vacuum impregnation of concrete using a fluorescent epoxy. The voids and cracks are filled up with fluorescent epoxy and so, it is possible to visualize the pore structure and crack propagation in concrete under UV light (Akyuz et al. 2007, Jakobsen et al. 2000).

In this paper, investigations on the uniaxial compressive behavior of concretes made with siliceous gravel and limestone are reported. For each aggregate type; the maximum particle size, the grading and water-cement ratio were kept constant but the volume fraction of aggregate in the mixtures was varied. After loading and unloading some of the specimens until the discontinuity and loosening limits, the plane section analyses were performed for better understanding the crack propagation under compression. Fracture energies under three point bending test were also obtained as a function of the aggregate volume fraction for both limestone and gravel aggregate concretes.

2 EXPERIMENTS

2.1 *Materials*

Local sand of the Istanbul area of 0-4 mm and the ordinary Portland cement (CEM I 42.5) were used. The specific gravity of this sand was 2.62 g/cm^3 and its water absorption was 0.80%. Two different coarse aggregates were used, the first one being a crushed limestone aggregate, and the second one was rounded siliceous gravel. The crushed limestone had a specific gravity of 2.70 g/cm^3 and water absorption of 0.5%. The specific gravity of the gravel was 2.58 g/cm^3 and its water absorption was 1.1%. Both the rounded siliceous gravel and crushed limestone were separated into two different size fractions such as 4/16 and 8/22 mm. The aggregate grading of all concretes was chosen between the ISO A32-B32 curves as shown in Table 1 and it was kept constant.

Table 1. Aggregate gradings used in the mixtures.

Sieve size, mm	22.0	16.0	8.0	4.0	2.0	1.0	0.5	0.25
Gravel	100	91	43	28	24	21	17	6
Crushed limestone	100	87	48	25	24	21	17	6

2.2 *Mixtures*

The maximum particle size of aggregate was kept constant at 22 mm. As seen in Table 1, the aggregate contents were increased with steps of 0.20 until 0.60 m^3/m^3 and mixtures with aggregate content of 0.73 m^3/m^3 were also produced. A mixture with only cement paste was also cast. Table 2 shows the mix proportions of the mixtures. The concrete mixtures had slumps between 10 mm and 230 mm. The concrete mixtures (M) produced were designated with the following codes: for limestone concretes CL and for gravel concretes G. The number after M shows the aggregate volume percentage.

Table 2. Mixture proportions (kg/m^3).

	M00	M20 G	M20 CL	M40 G	M40 CL	M60 G	M60 CL	M73 G	M73 CL
Cement	1643	1295	1291	968	963	631	634	405	399
Water	460	363	362	271	271	177	177	101	100
Admixture	0	0	0	0	0	1.5	0.9	6.6	4.8
F.A.	0	130	128	262	261	385	392	465	459
C.A. (4-16 mm)	0	247	240	498	487	730	731	882	858
C.A. (8-22 mm)	0	139	161	282	326	414	490	500	574
Density	2093	2174	2141	2282	2308	2347	2430	2379	2409

F.A.: fine aggregate (0-4 mm)
C.A.: coarse aggregate (gravel or crushed limestone)

For the mixtures containing coarse aggregates up to 60%, the water/cement ratio was kept at 0.28. However, the mixtures with aggregate content of 73% were produced with water/cement ratio of 0.25. A superplasticizer was used in the concrete mixtures containing high aggregate volume fractions of 0.60 and 0.73 m^3/m^3. Mixtures were prepared in a small laboratory mixer with vertical rotation axis by forced mixing. The concretes were placed in cylindrical moulds of 150 mm diameter and 300 mm height. Prisms of 100x100x500 mm were also cast.

2.3 *Testing*

Compressive strength and modulus of elasticity are measured on cylindrical specimens of 150 mm in diameter and 300 mm in height. The static moduli of elasticity were calculated from the ascending part of the stress-strain curves in compression for stresses below approximately 30 percent of the ultimate strength using least squares method.

The same specimens were also used to determine Poisson's ratios by measuring both the axial and lateral strains in compression. Based on these measurements, the discontinuity and loosening limits of the specimens were calculated.

After determining the discontinuity and loosening limits, three other cylinder specimens were loaded until the discontinuity and loosening limits, then unloaded. Samples of 10 x 20 cm were cut out from these cylinder specimens parallel to loading axes and then impregnated under vacuum with a yellow fluorescent epoxy. Thus, the capillary pores, cracks, voids, and defects in the concrete are filled with epoxy. After impregnation, the plane and thin sections were polished and inspected under UV light using an optical microscope.

Three-point bending tests were performed on the beams of 100x100x500 mm size, the support span being 400 mm. The beam specimens contained notches at the mid span which were obtained by cutting with a diamond saw. Two notch depths, 1 cm and 5 cm, were used in this study. The deflection rate at the middle of the beams was kept constant at 0.02 mm/min. The load was applied by a closed-loop testing machine of 100 kN capacity, and the deflections were measured simultaneously by using LVDTs. Thus, the load versus deflection curve for each beam was obtained by recording measurements taken at the mid point. Four beams were tested for each mixture.

3 RESULTS AND DISCUSSION

3.1 *Mechanical Properties*

The mechanical properties of the mixtures are given in Table 3.

As seen in Table 3, the moduli of elasticity of the mixtures containing gravel are almost the same as that of the hcp mixture up to 40% but beyond this amount, the values increased. For the mixtures containing crushed limestone aggregate, the modulus of elasticity increased as the volume fraction of this aggregate is increased. The modulus of elasticity of aggregates is higher than that of hcp. Thus, the modulus increases with aggregate concentration. On the other hand, for the aggregate concentration of 73%, the modulus of elasticity of the mixture produced with crushed limestone is about 1.5 times higher than that of the mixture with gravel. It is known that the modulus of elasticity of siliceous rocks is greater than that of calcareous rocks. On the other hand, it is seen that the interface zone is weaker for gravels. Then, it can be thought that, even at stresses below 30 percent of the compressive strength, noticeable crack openings occur in gravel – cement paste interfaces which are sufficient for decreasing the modulus of elasticity.

Table 3. Mechanical properties.

Mix Code	Compressive strength (MPa)	Modulus of elasticity (GPa)	Poisson's Ratio	Splitting tensile strength (MPa)
M00	53.8	23.1	0.29	3.15
M20G	45.9	22.2	0.26	4.05
M40G	41.7	23.5	0.21	4.80
M60G	40.2	28.7	0.19	6.30
M73G	38.2	29.7	0.19	7.55
M20CL	49.1	22.1	0.26	4.10
M40CL	46.3	32.3	0.28	4.15
M60CL	64.5	38.5	0.30	4.65
M73CL	66.3	44.7	0.30	5.80

The Poisson's ratios given in Table 3 were obtained at 40% of the ultimate load and as seen in this table, the Poisson's ratios of the concretes containing gravel are lower compared to crushed limestone aggregates. For the limestone aggregate concretes, the relation between Poisson's ratio and the aggregate volume fraction has a minimum around 0.20 m^3/m^3. For the concretes with gravel aggregates, Poisson's ratio decreases with increasing the aggregate volume fraction (Fig. 1).

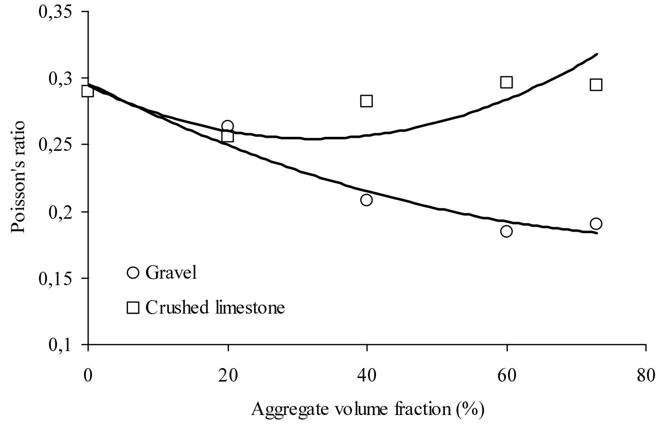

Figure 1. Effect of aggregate volume fraction on Poisson's ratio.

As seen in Figure 2, as the compressive strength of concrete increases, at the beginning Poisson's ratio increases significantly. Above 50 MPa, however, Poisson's ratio increases slightly. In concretes with gravel aggregates, low values of Poisson's ratio are obtained compared to those of concretes with limestone. Similar results were reported by Tasdemir & John (1987).

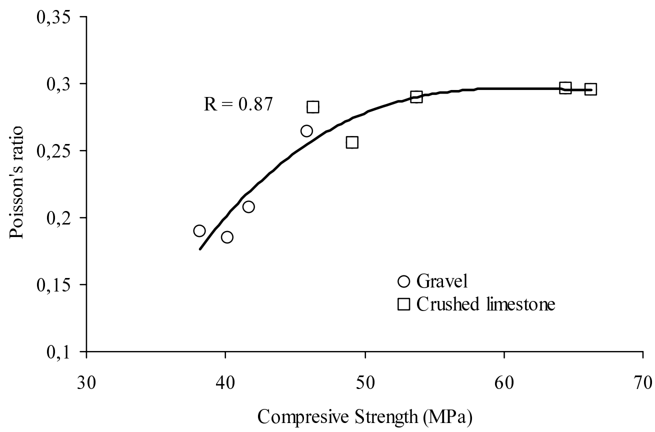

Figure 2. Effect of compressive strength on Poisson's ratio.

Splitting tensile strengths of the concretes are also shown in Table 3. With increasing coarse aggregate concentration, higher splitting strength values were obtained. In these mixtures, cracks are forced by the state of stress to travel through the aggregate and since the tensile strength of coarse aggregate is greater than that of the matrix, greater splitting-tensile strength is obtained.

3.2 *Critical Stresses and Compressive Strength*

The discontinuity limit is defined as the point at which the ratio of the lateral strain to the longitudinal strain begins to increase significantly. This is equivalent to the point at which Poisson's ratio starts to increase (Dragon & Mroz 1979). Above the discontinuity limit microcracking increases significantly, and then at a certain stress, the volume of specimen begins to increase rather than continue to decrease, this critical stress can be defined as the loosening limit. The discontinuity and loosening limits are schematically shown in Figure 3.

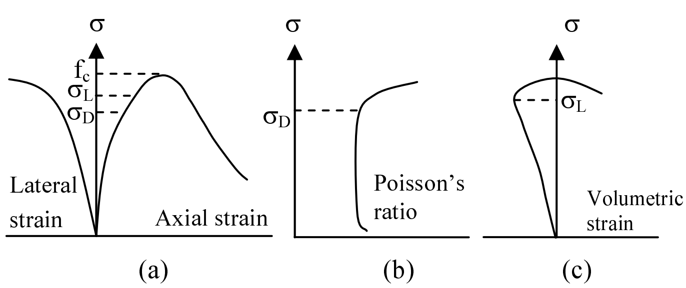

Figure 3. Schematic representation of stress vs. (a) longitudinal and lateral strain, (b) Poisson's ratio, and (c) volumetric strain.

Figure 4 and 5 show the effect of aggregate volume fraction on the discontinuity and loosening limits of concrete, respectively. As seen in these figures, the discontinuity and loosening limits decrease gradually for the mixtures with gravel aggregates. For the mixture with crushed limestone aggregate however, both the discontinuity and loosening limits decrease slightly up to an aggregate volume fraction of approximately 40%, but beyond this value, substantial increases were recorded.

The test results show that the ratio of the discontinuity stress to the compressive strength is between 82% and 87% for gravel, and between 84% and 92% for crushed limestone. The ratio of loosening stress to the compressive strength is between 86% and 93% for gravel, and between 94% and 96% for crushed limestone. These ratios are much higher than those of lower strength concretes. This fact reflects the brittleness which occurs by the increasing of the strength.

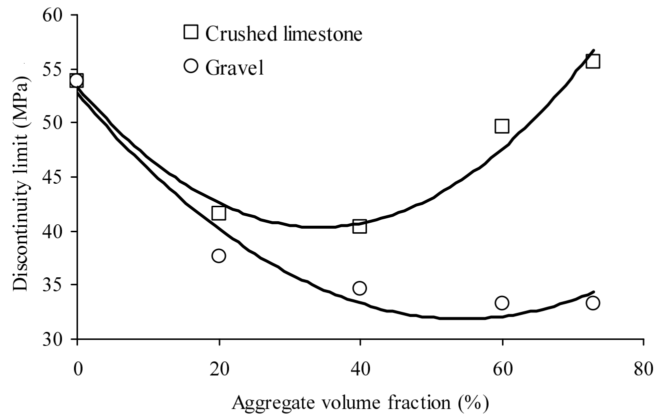

Figure 4. Effect of aggregate volume fraction on discontinuity limit.

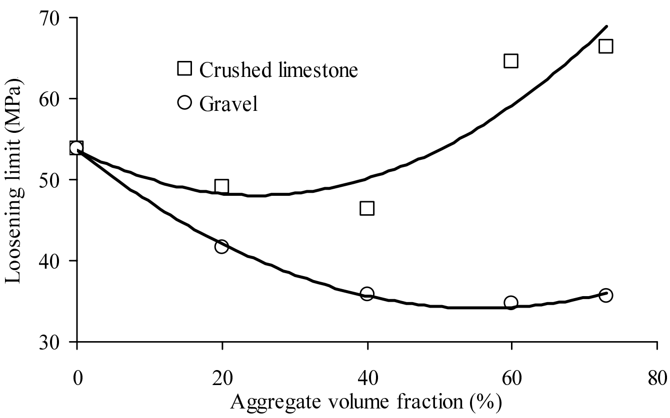

Figure 5. Effect of aggregate volume fraction on loosening limit.

Figure 6 shows the effect of aggregate concentration on the compressive strength of concrete. In gravel concretes, the compressive strength decreases with the increase in gravel concentration. For the mixtures containing crushed limestone, a reduction was recorded up to 40%, however, beyond this limit compressive strength increased.

The gradual strength reduction in mixtures containing gravel may be due to the increased number of interfaces between the aggregate and hardened cement paste. It is well established that the interface is the weakest link in concrete and as the amount of interfaces increase, strength reductions can be expected. In addition, the gravel has a smooth surface which causes a weaker interface. After testing, the examinations on the fractured planes indicate the cracks usually travelled around the gravel aggregates. In concretes containing crushed limestone aggregates, however, cracks usually forced through the aggregates. Thus, these aggregates produce an obstacle for crack propagation. Beyond the aggregate concentration of 0.40 m^3/m^3, this obstacle effect dominates the weakening effect caused by the new interfaces of added aggregates. Thus, the compressive strength increases.

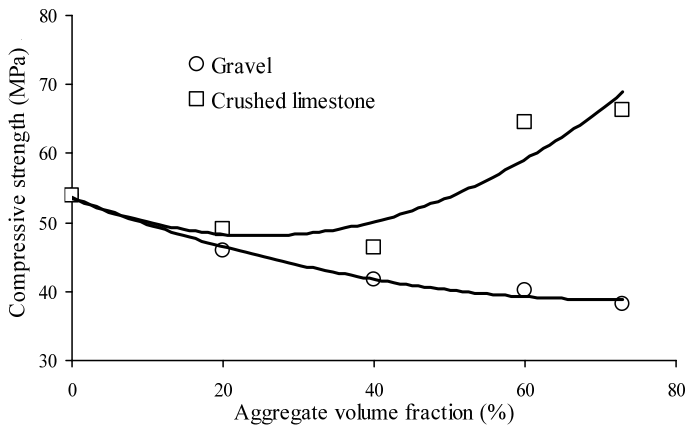

Figure 6. Effect of aggregate volume fraction on compressive strength.

Tasdemir et al. (1990) studied the crack initiation and propagation on mortar blocks with rectangular model aggregate under uniaxial compression. During the experiments, it was possible to observe crack initiations, crack extension and to obtain the load versus crack extension curve, main crack tip displacements and propagating crack face displacements using laser holography. The experimental study showed that a bond crack always proceeded the initiation of a mortar crack. Moreover, along the crack generated in the mortar, the study revealed that both opening (tensile) and sliding displacement did occur, but the opening mode was dominant during the crack propagation.

The decreasing trend of strength in gravel aggregate concrete observed up to the value of 0.40 m^3/m^3, can be explained by a model proposed by Akyuz (1990). In this model, as seen in Figure 7, circular inclusions were arranged with respect to the regular hexagonal symmetry in an infinite plate. The inclusions were all of equal radii and their centers were located at the center of the hexagons. In a representative region of the plate, stress distributions were calculated using the collocation theory under far field uniform loads. In the polar coordinate system, the domain of the stress functions for the dispersed phase is the circular area of radius r_o with the center at the origin. Likewise, for the matrix phase, it is the ring area between the circle with the radius r_o and the boundary defined by ABCDEFGHIJKLA. The stress functions belonging to these domains were obtained by Akyuz (1990) taking into consideration the far field uniform loading conditions. It was shown that the results calculated according to the theory were very close to the results obtained by the exact solution in case of single inclusion, where several fracture planes may develop parallel to the loading axes in the three-dimensional case. When the composite material is under far field uniform loads in the x or y direction, the average stresses on the hexagonal unit cell equal to following stresses. This can be expressed as:

$$\frac{1}{S_0}\int_{S_1+S_2}\sigma_{yy}dS = 1 \quad \text{and} \quad \frac{1}{S_0}\int_{S_1+S_2}\sigma_{xx}dS = 0 \qquad (1)$$

The integration regions S_1 and S_2 are defined as follows: S_1={the area between the circle with the radius r_0 and the regular hexagon PQRSTZ}, $S_2=\{0\leq r \leq r_0 , 0 \leq \theta \leq 2\pi\}$. S_0 is the surface area of unit cell.

It is assumed that there is perfect bonding between the circular zone with a radius of r_0 (dispersed phase) and the ring zone for $0 \leq \theta \leq 2\pi$.

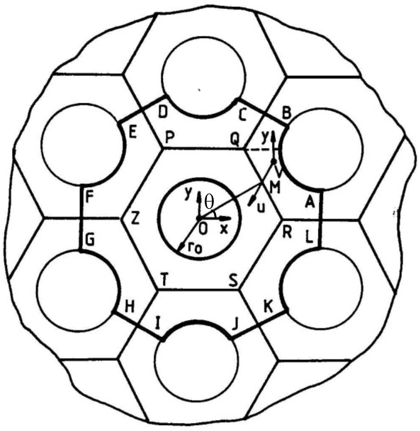

Figure 7. Circular inclusions with respect to the regular hexagonal symmetry (Akyuz 1990).

Based on the Akyuz's model (1990), it can be concluded that the stress concentrations increase at the weak matrix-aggregate interfaces as the volume fraction of aggregate in the mixture increases. This increase in stress concentration may be responsible of the drop of the compressive strength.

For the volume fractions greater than 0.40 m^3/m^3, the number of limestone aggregates in the vertical cross sectional planes reaches a sufficient level. At the stress level of loosening limit or above this critical stress, the vertical cracks grow through the aggregates and since the strength of limestone aggregate is greater than that of the matrix, the compressive strength of limestone aggregate concretes slightly increases. Although there is augmentation of stress concentrations at the matrix-aggregate interfaces, however, the beneficial effect rising from the cracks growing through the aggregates is dominant. Hence, above the loosening limit vertical cracks pass through the aggregates and as a result, transgranular type of fracture occurs.

For the rounded siliceous gravel aggregates, as seen in Figures 4, 5 and 6, the critical stresses (i.e. σ_D and σ_L) and compressive strength decrease with increasing the volume fraction of aggregates. In these concretes, the weak interface between aggregate and matrix, and the increase in the stress concentrations cause decrease in σ_D and σ_L and also in compressive strength as the volume fraction of aggregate increases.

After completion of the compression tests, the fracture surfaces were examined, in concretes with siliceous aggregates, the cracks usually travelled around the aggregates and the smooth matrix-aggregate interface fractures were observed. Shah & Chandra (1968) have made similar conclusions for the gravel aggregate concretes. For the gravel aggregate concretes Amparano et al. (2000) have shown that in the range of aggregate volume fraction between 65 and 75%, compressive strength of concrete decreases slightly with increasing the aggregate volume fraction. In concretes of CL series, however, cracks usually forced through the aggregates, as a result the critical stresses and compressive strength increased after the minimum value.

3.3 *Fracture Energies*

By using a closed loop testing machine, the descending branches of the beams were also obtained at the three point bending test. Figure 8 shows the load - displacement curves of the mixtures containing gravel. These results were obtained for the notch depth of 5 cm. Based on the test results, fracture energy (G_F) of the beams were obtained according to Equation 2:

$$G_F = \frac{W_o + mg\delta_o}{A_{lig}} \qquad (2)$$

where W_o is the the area under load versus deflection curve, m is the mass of the beam, g is the gravitational acceleration, δ_o is the deflection of the beam and A_{lig} is the effective cross section of the beam.

Table 4 summarizes the fracture properties of the mixtures. As seen in the table, the fracture energies increased with the aggregate volume fraction. For the aggregate concentration of 20%, the fracture energy of the mixtures containing crushed limestone is higher and the results for the 40% concentration are almost the same for both types of aggregates. For higher aggregate concentrations, however, mixtures containing gravel have higher fracture energy.

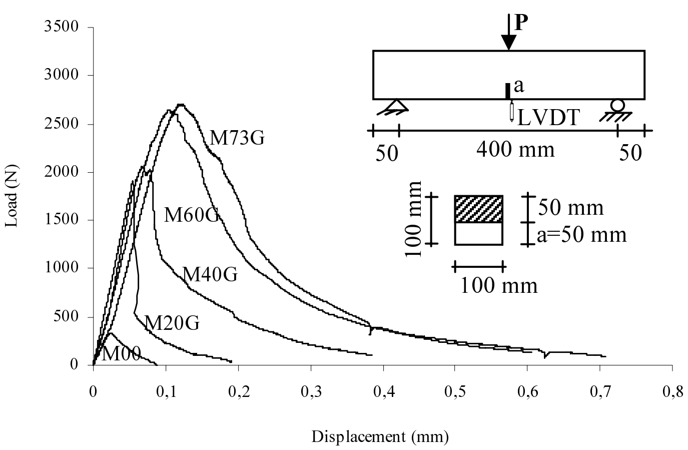

Figure 8. Load – displacement curves for the mixtures containing gravel (depth of the notch is 50 mm).

Table 4. Fracture properties of the mixtures.

		Aggregate volume fraction				
		0%	20%	40%	60%	73%
Fracture energy (N/m)						
Gravel	5 cm notch	9.6	23.6	50.0	97.4	115.1
	1 cm notch	14.2	43.4	73.2	137.0	150.9
Crushed	5 cm notch	9.6	40.8	50.0	57.7	56.7
Limestone	1 cm notch	14.2	61.2	68.1	79.3	88.0
Characteristic length (mm)						
Gravel	5 cm notch	22	32	51	70	60
	1 cm notch	33	59	75	99	79
Crushed	5 cm notch	22	54	94	103	75
Limestone	1 cm notch	33	80	128	141	117

Fracture energy of the specimens containing notches of 5 cm depth is shown in Figure 9.

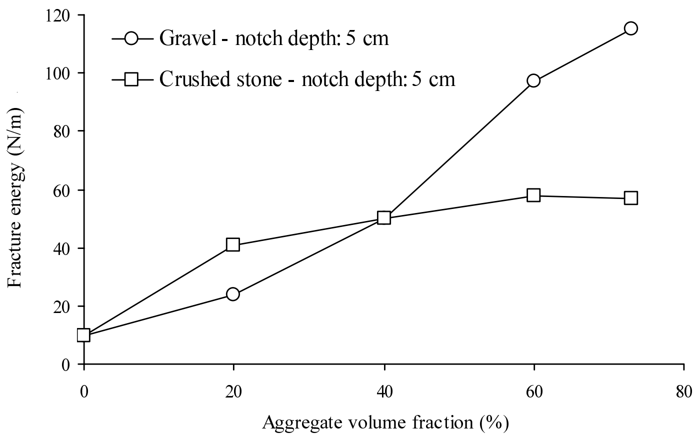

Figure 9. Fracture energy of the mixtures containing 5 cm notch.

Test results indicate that for the 60% and 73% aggregate concentrations, the increase in fracture energy with aggregate volume fraction is more substantial for the mixtures containing gravel. For example, for the aggregate volume fraction of 60% and specimen notch depth of 5 cm, the fracture energy of the mixture with gravel is about 70% higher than that of the one with crushed limestone.

In gravel concretes, the crack usually does not traverse the aggregate due to its rounded shape and smooth surface, hence crack path is longer and fracture is less brittle. In limestone concretes, however, the cracks usually travel through the aggregate, and fracture tends to be brittle in nature. This different crack pattern in limestone concretes can be attributed to the interfacial zone becoming stronger and more homogeneous, thus material exhibits a more brittle behavior and transgranular type of fracture leads to lower fracture energy compared to those of gravel concretes.

From the evaluation of fracture energy (G_F) in Figure 9, ranging from brittle hardened cement paste to real concrete, characteristic length (l_{ch}) can be calculated as;

$$l_{ch} = \frac{G_F.E}{f_t^2} \tag{3}$$

where E is the modulus of elasticity and f_t is the tensile strength of concrete. The characteristic lengths calculated are shown in Figure 10 for the notch depths of 5 cm. The characteristic lengths calculated are also shown in Table 4. Characteristic length of the mixtures increase with increasing aggregate volume content.

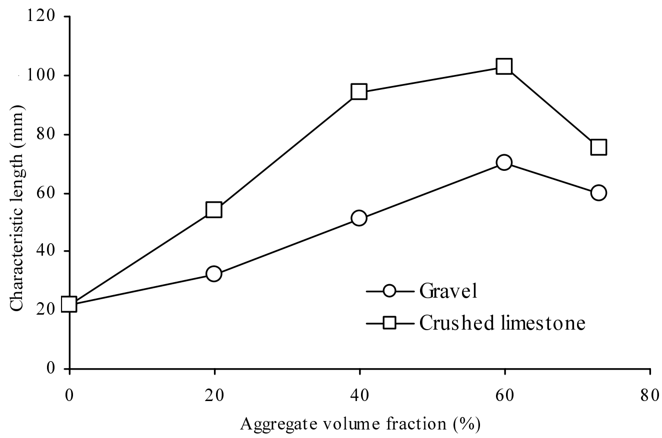

Figure 10. Characteristic length of the mixtures containing 5 cm notch.

Recent research shows that net bending strength, splitting tensile strength and the characteristic length (which is used for the indication of the ductility of concrete) increases substantially with increasing aggregate volume fraction (Tasdemir&Karihaloo 2001, Tasdemir et al. 2004). For higher aggregate volume fraction, since the increase of splitting tensile strength is high, l_{ch} shows decreasing trend with respect to the aggregate volume fraction.

3.4 *Microstructural Studies*

Some of the cylinder specimens were loaded up to the discontinuity and loosening limits to propagate cracks within the specimens. For investigating the intergranular or transgranular type of fractures in concrete made with two different aggregates, plane sections of the samples were prepared. For this purpose, samples with cross-sectional area of 10x20 cm were cut and impregnated with fluorescent epoxy under vacuum. The fluorescent in the epoxy enters the micro-cracks and macro-cracks, capillary, entrained and entrapped air voids, starting from the surface of the specimen. Since the sample is polished and inspected under UV light, it is possible to see the pore structures, and micro- and macro-cracks. Figure 11 shows the plane section image of the limestone concrete sample with the volume fraction of 0.60.

Figure 12 shows plane sections of concretes with gravel aggregates for the aggregate volume fractions of 0.40 and 0.60 m^3/m^3. As seen in this figure, vertical cracks travel around the aggregates and intergranular type of fracture occur.

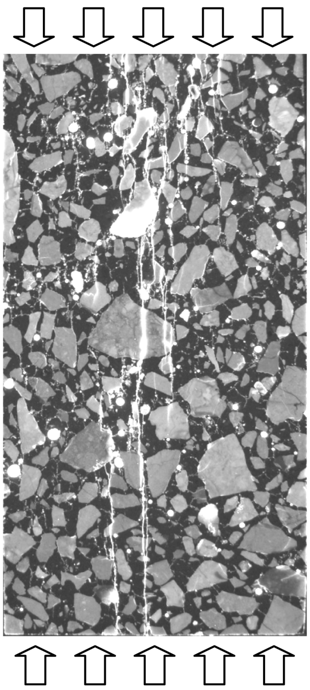

Figure 11. Plane section of the mixture containing 60% limestone aggregate loaded until loosening limit.

For the thin section analysis, the sample preparations are similar to the ones for the plane section. After impregnation of the specimen with fluorescent epoxy, thin sections are prepared from slices of concrete that are attached to a glass slide, and then ground to a thickness of about 20μm to 30μm. These thin sections give an opportunity to identify the material constituents and predict their proportions, air content, water-cement ratio, paste homogeneity, paste volume, aggregate volume, effectiveness of curing, and studying the relationships between the various constituents (Akyuz et al. 2007).

Based on the thin section studies, the following results are obtained: Figure 13a shows that typical intergranular type of fracture occurs above the loosening limits of gravel concretes with aggregate volume fraction of 0.60 m^3/m^3, however, the transgranular type of fracture is observed in limestone concretes with aggregate volume fraction of 0.40 m^3/m^3 (Fig. 13b).

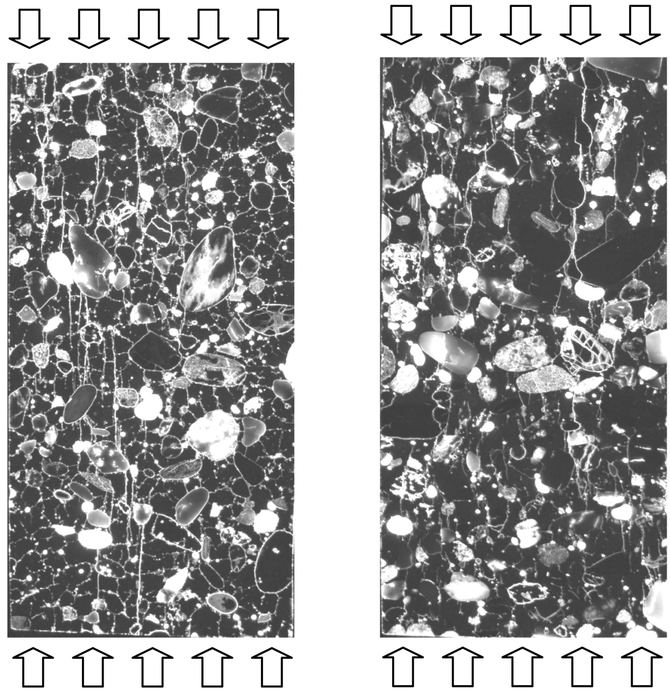

(a) (b)

Figure 12. Plane section of the mixture containing (a) 40% (b) 60% rounded siliceous aggregate loaded until loosening limit.

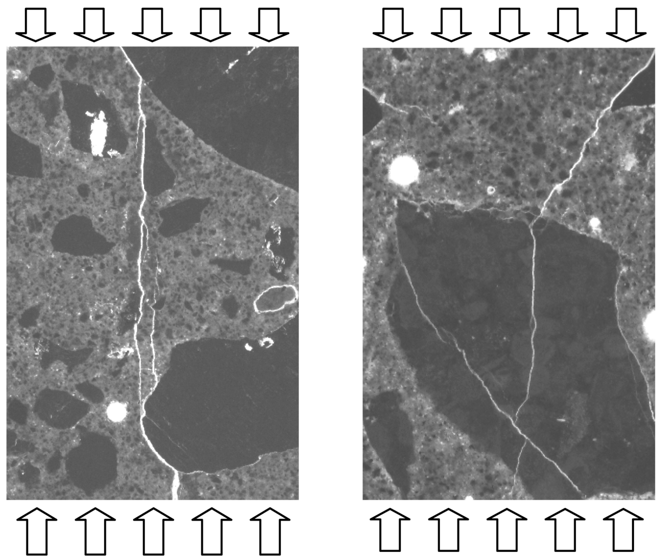

(a) (b)

Figure 13. Thin sections of the mixture containing (a) 60% gravel (b) 40% crushed limestone aggregate (50x).

4 CONCLUSIONS

The results obtained from this study can be summarized as follows:

1) Critical stresses (i.e. discontinuity and loosening limits) and compressive strength of limestone concrete decrease with an increase in the aggregate

volume fraction up to a value of about 0.40m^3/m^3, then it increases slightly. In gravel concretes, however, critical stresses and compressive strength decrease continuously as the aggregate volume fraction increases. In gravel concretes, the smooth surface of the aggregates play a negative role in compression where several fracture planes may develop parallel to loading axes, finally an intergranular type of fracture occurs. In limestone concretes, however, cracks usually forced through the aggregates, as a result the fracture of these concretes becomes in transgranular manner. Microstructural examinations on plane sections and also thin sections confirm these results.

2) For the limestone aggregate concretes, Poisson's ratio has a minimum value around 0.20 m^3/m^3. In gravel aggregate concretes, however, Poisson's ratio decreases with increasing the aggregate volume fraction. In addition, Poisson's ratio increases with increasing compressive strength of concrete for both limestone and gravel concretes. The modulus of elasticity of concrete increases with increasing aggregate volume fraction. This increase in limestone concretes is more noticeable compared to those of gravel concretes.

3) In both gravel and limestone concretes, as the aggregate volume fraction increases, the splitting tensile strength increases significantly.

4) As the volume fraction of aggregate in the mixture increases, fracture energy of concrete increases significantly. Compared to crushed limestone, gravel aggregate concrete has a more pronounced effect in increasing the fracture energy especially in high volume fraction of aggregate. Characteristic length also increases with increasing the aggregate volume fraction but for highest aggregate volume fractions it tends to decrease. Thus, the results obtained give a clear quantitative picture of how brittle matrix (hcp) progressively transforms into a tougher, stiffer and more ductile concrete as the aggregate volume fraction increases.

ACKNOWLEDGEMENT

This research was completed in the Faculty of Civil Engineering at Istanbul Technical University. The authors also wish to acknowledge the financial support of TUBITAK (The Scientific and Technological Research Council of Turkey) Project: 106G122, 1007-Kamu.

REFERENCES

Amparano F. E., Yunging X. & Young-Sook R. 2000. Experimental Study on the Effect of Aggregate Content on Fracture Behavior of Concrete. *Engineering Fracture Mechanics* 67: 65-84.

Akyuz, S. 1990. A Solution of the Problem of Circular Inclusions with the Regular Hexagonal Symmetry in Finite Plate In *6th National Mechanics Congress*, Vol.1, pp.86-93 (in Turkish with English Abstract).

Akyuz, S., Akkaya, Y., Yazan, H.O. & Tasdemir, M.A. 2007. Damage Mechanics Based Modelling of the Relation Between Capillary Pores and Compressive Strength of Concrete. In Carpinteri et al. (Eds) *Fracture Mechanics of Concrete and Concrete Structures* Taylor & Francis Group, London. 1783-1788.

Dragon, A. & Mróz, Z. 1979. A Continuum Model for Elastic-Brittle Behaviour of Rock and Concrete. *International Journal of Engineering Science* 17: 121-137.

Jakobsen, U.H., Laugesen, P. & Thaulow, N. 2000. Determination of Water-Cement Ratio in Hardened Concrete by Optical Fluorescence Microscopy. In *Water-Cement Ratio and Other Durability Parameters – Techniques for Determination*. ACI SP-191: 27-41.

Jensen, A.D. & Chatterji S. 1996. State of the art report on micro-cracking and Lifetime of Concrete-Part 1, TC-122-MLC: Micro-cracking and Lifetime Performance of Concrete. *Materials and Structures* 29: 3-8.

Konsta-Gdoutos, M.S. (editor). 2006. Measuring, Monitoring and Modeling Concrete Properties, *Proc. Int. Symp. Dedicated to S.P. Shah* Springer, 786 p.

Shah, S.P. & Chandra S. 1968. Critical Stress, Volume Change and Microcracking of Concrete. *ACI Journal* September: 770-781.

Shah, S.P., Ouyang, C. & Swartz , S.E. 1995. *Fracture Mechanics of Concrete*. New York, John Wiley and Sons Inc.

Shah, S.P. & Tasdemir, M.A. 1994. Role of Fracture Mechanics in Concrete Technology. In V.M. Malhotra (ed), *Advances in Concrete Technology:* 161-202, CANMET, Second Edition.

Tasdemir,M.A., Akyuz, S., Bayramov, F., and Agar, A.S. 2004. Inclusion Based Modelling of Concrete with Various Aggregate Volume Fraction. In *Continuum Models and Discrete Systems (CDMS)*, Kluver Academic Publisher, 253-258.

Tasdemir, M.A. & John, R. 1987. Discussion of the Paper "Elastic Modulus, and Poisson's Ratio of Concrete" by Klink S.A., *ACI Materials Journal* 84(6): 562-566.

Tasdemir, M.A., Maji, A.K. & Shah,.S.P. 1990. Crack Propagation in Concrete under Compression. *Journal of Engineering Mechanics* 116(5): 1058-1076.

Tasdemir, C., Tasdemir, M.A., Mills, N., Barr, B.I.G. & Lydon, F.D. 1999. Combined Effects of Silica Fume, Aggregate Type, and Size on Post-Peak Response of Concrete in Bending. *ACI Materials Journal* 96(1): 74-83.

Tasdemir, M.A. & Karihaloo, B.L. 2001. Effect of Aggregate Volume Fraction on the Fracture Parameters of Concrete: A Meso-Mechanical Approach. *Magazine of Concrete Research* 53(6): 405-415.